DOI: 10.1002/ange.201210226

Oxidation of Water

A Tailor-Made Molecular Ruthenium Catalyst for the Oxidation of Water and Its Deactivation through Poisoning by Carbon Monoxide**

*Markus D. Kärkäs, Torbjörn Åkermark, Hong Chen, Junliang Sun, and Björn Åkermark**

The transition to new sustainable energy sources is one of the greatest challenges facing the human society today.[1] Overall H_2O splitting, employing distinct catalysts and solar energy, has been a central issue for the scientific community during the past decades because of its potential of producing green and renewable energy, for example, molecular hydrogen. The splitting of H_2O can thus be divided into two half-reactions; the oxidation of water and the reduction of protons. The fact that the former half-reaction requires highly oxidizing conditions, makes H_2O oxidation more troublesome and discovering catalysts for this transformation is highly challenging and is thus far the limiting step and the linchpin for durable artificial photosynthetic systems.

The oxidation of H_2O to O_2 is complex, in that it invokes the consecutive removal of four electrons and reshuffling of several bonds to finally liberate O_2. During three billion years, nature has evolved and fine-tuned a sophisticated system to achieve photocatalytic H_2O oxidation. In this multi-step process, solar energy is harnessed to convert simple starting materials into valuable feed stocks for biological organisms. At the heart of PS II is the oxygen evolving complex (OEC), containing the catalytically active Mn_4Ca-core[2] which manages to catalyze the oxidization of H_2O to O_2 at a tremendous rate and with a high turnover, thus reflecting considerable stability. Nonetheless, even this system is degraded and continuously has to be reassembled.

Thus far, the artificial water oxidation catalysts (WOCs) are decidedly less stable, although there have been significant advances during the last decade.[3] The intensive quest for a viable WOC has contributed to a range of heterogeneous,[4] homogeneous,[5–9] and also some examples of immobilized homogeneous catalysts.[10] The prevailing homogeneous WOCs consist of complexes of Ru[5] and Ir[6] from the second and third row, respectively, and recently complemented by complexes of the first-row transition metals Mn,[7] Fe,[8] and Co.[9]

Under the highly oxidizing conditions required to oxidize H_2O, the WOCs are decomposed and/or deactivated after a certain time period. This is a serious and general issue encountered with WOCs and insight into the deactivation pathways is necessary if more stable WOCs are to be realized. The current information regarding the deactivation of molecular WOCs is quite dispersed and ligand dissociation[5g] and oxidative decomposition[11] have been pointed out as the main deactivation pathways.

Ligand architecture and catalyst optimization are of primary importance for developing WOCs with a longer lifetime. The main obstacle encountered with the majority of WOCs is the high oxidation potentials required to achieve H_2O oxidation. One way of overcoming this problem is to introduce anionic ligands to stabilize and lower the high oxidation potentials.[5d,f,12] Recently, we employed a bioinspired strategy to synthesize ligands of this type, for the development of single-site ruthenium complexes which showed high activity in the oxidation of H_2O with the mild oxidant $[Ru(bpy)_3]^{3+}$.[5f] Inspired by this work it was thus envisioned that a tailored catalyst design based upon the tetradentate ligand scaffold rendered by ligand **3** [H_2bpb = *N*,*N*′-1,2-phenylene-bis(2-pyridine-carboxamide)] would afford highly versatile ruthenium-based WOCs. The readily accessible tetradentate ligand scaffold **3** offers an easily modified ligand environment, an important factor for tuning WOCs and for the construction of supramolecular assemblies.

Herein we report two single-site ruthenium complexes, based upon the tetradentate ligand **3**, **4** ($[Ru(bpb)(pic)_2]Cl$) and **5** ($[Ru(bpb)(CO)(OH_2)]$) (Figure 1), which despite structural similarities display a remarkable difference in their catalytic and chemical behavior. During catalytic H_2O oxidation by **4**, complex **5** is generated. This contains a coordinated carbon monoxide (CO) molecule and proved to be inactive in H_2O oxidation when using $[Ru(bpy)_3]^{3+}$ as oxidant. CO is one of the gaseous byproducts generated by oxidative decomposition (either from the catalyst itself or from $[Ru(bpy)_3]^{3+}$-type complexes, both pre-generated and photo-

[*] Dr. M. D. Kärkäs, Prof. B. Åkermark
Department of Organic Chemistry, Arrhenius Laboratory
Stockholm University
10691 Stockholm (Sweden)
E-mail: bjorn.akermark@organ.su.se
Dr. T. Åkermark, Prof. J. Sun
Department of Materials and Environmental Chemistry
Arrhenius Laboratory, Stockholm University
10691 Stockholm (Sweden)
H. Chen
Berzelii Center EXSELENT on Porous Materials and
Department of Materials and Environmental Chemistry
Arrhenius Laboratory, Stockholm University
10691 Stockholm (Sweden)
and
Faculty of Material Science and Chemistry
China University of Geosciences
Wuhan 430074 (P.R. China)

[**] This project was supported by the Swedish Energy Agency, the Knut and Alice Wallenberg Foundation, the Swedish Research Council (VR), and the Swedish Governmental Agency for Innovation Systems (VINNOVA) through the Berzelii Center EXSELENT. H.C. would also like to thank the China Scholarship Council for his scholarship.

Supporting information for this article is available on the WWW under http://dx.doi.org/10.1002/anie.201210226.

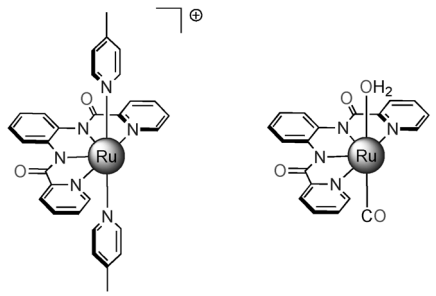

4 5

Figure 1. Molecular structures of the single-site ruthenium complexes **4** and **5**.

chemically generated) during the catalytic oxidation of H_2O. This catalytic difference suggests a novel, and maybe general, pathway for deactivation of ruthenium-based WOCs. This is a key observation because thus far CO has been considered as an innocent spectator molecule but our results imply that it can contribute to the deactivation of ruthenium-based WOCs during catalytic H_2O oxidation.

Ligand **3**[13] was synthesized from 1,2-phenylenediamine (**1**) and 2-pyridinecarboxylic acid (**2**) by use of triphenyl phosphite as coupling reagent. The corresponding single-site ruthenium complex **4** was obtained by refluxing with $[Ru(DMSO)_4Cl_2]$, in the presence of Et_3N and 4-picoline (see the Supporting Information for further details). The structure of complex **4** was confirmed by high-resolution mass spectrometry (HRMS), NMR spectroscopy, and UV/Vis spectroscopy.

Evaluation of the catalytic activity toward the chemically driven oxidation of water for complex **4** was carried out with $[Ru(bpy)_3]^{3+}$ as chemical oxidant in a buffered aqueous solution (0.1 M phosphate buffer, pH 7.2) and is depicted in Figure 2 and Figure S5. The primary advantage of employing this oxidant is its activity at near-neutral conditions, compared to Ce^{IV} which requires acidic pH. However, only a few WOCs have been characterized, employing $[Ru(bpy)_3]^{3+}$ as oxidant, probably because of the high oxidation potential required to activate a majority of the reported WOCs, with a few molecular ruthenium-based catalysts and inorganic polyoxometallates being the notable exceptions.[5d,f,14]

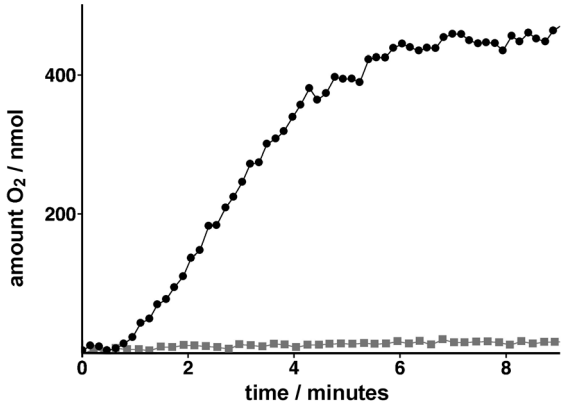

Figure 2. Kinetic curves for the evolution of O_2 by complex **4** (●) and **5** (■) versus time. Conditions: An aqueous phosphate buffer solution (0.1 M, pH 7.2, 0.5 mL) containing the complex (30 μM) was added to the oxidant $[Ru(bpy_3)](PF_6)_3$ (3.0 mg, 3.0 μmol).

Upon the addition of an aqueous solution of complex **4** to the oxidant, gas bubbles were immediately observed. Real-time mass spectrometry measurements enabled us to confirm the evolution of O_2 and the high activity expressed by complex **4** (turnover number, TON = 200; turnover frequency, TOF ≈ 0.12 s^{-1}). Control experiments were also carried out to establish the catalytic importance of complex **4**, where an equimolar amount of RuO_2 was used instead of complex **4**. This resulted in negligible amounts of produced O_2, thus confirming the importance of complex **4**.

Detailed studies were carried out to probe the stability of complex **4** towards ligand dissociation and oxidative decomposition. It is bench-stable and can be stored under an air atmosphere without any detectable decomposition. Complex **4** is also hydrolytically stable in the range $1 < pH < 7$ for at least seven days at ambient temperature. This was confirmed by examination of the UV/Vis absorption spectra as well as by NMR spectroscopy (Figures S24–S27).

To provide further support that complex **4** is the active catalyst during the oxidation of H_2O and that it retains its identity after catalytic cycling, a solution of the reaction mixture after about 20 turnovers was analyzed by HRMS (see the Supporting Information for details). This resulted in the appearance of a peak, in positive mode, at $m/z = 604.1149$ which is ascribed to $[Ru(bpb)(pic)_2]^+$ (Figure S13). This shows that the structure of the catalyst is retained.

The reaction mixture was also examined by HRMS after the O_2 evolution had ceased. A major peak at $m/z = 462.9985$ was observed, in negative mode, corresponding to $[Ru(bpb)(CO)(OH_2)$ (**5**)$-H^+]^-$ (Figure S14). The fact that in addition to the evolution of O_2, CO is generated as one of the gaseous reaction byproducts (by decomposition from the catalyst itself or from the oxidant $[Ru(bpy)_3]^{3+}$) during the H_2O oxidation experiments and explains the formation of complex **5** from **4**. A probable intermediate in the conversion of complex **4** into **5** could also be found (in positive mode) at $m/z = 539.0548$ corresponding to $[Ru(bpb)(pic)(CO)]^+$ (Figure S15).

These findings indicate that complex **5** is not an active catalyst for H_2O oxidation. To verify this, complex **5** was separately synthesized by refluxing ligand **3** in *N*,*N*-dimethylformamide in the presence of $RuCl_3$, and KH as base, with in situ generation of CO by thermal decomposition of *N*,*N*-dimethylformamide (see the Supporting Information for further details). X-ray quality single-crystals were grown by slow diffusion of a toluene solution into a methanol solution containing **5**. The crystal structure of complex **5** is depicted in Figure 3. In complex **5**, the ruthenium atom is in a six-coordinate configuration, with the tetradentate ligand **3** bound to the ruthenium center together with a H_2O molecule and carbon monoxide occupying the axial positions. The angle of N1-Ru1-N4 is 115.0°, and larger than the ideal 90° of an octahedral configuration and may supply a seventh coordination site for complexes containing ligand **3**. The details of selected angles and bond lengths can be found in the Supporting Information in Table S1, together with the structure of the hydrogen-bonding network (Figure S16).

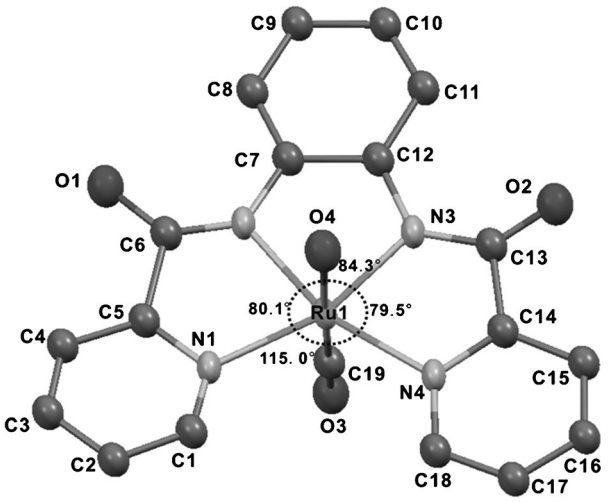

Figure 3. Crystal structure of complex **5** with thermal ellipsoids at 30% probability. Hydrogen atoms and solvent are omitted for clarity.

For a detailed discussion regarding the coordination properties of the two ruthenium complexes see the Supporting Information.

The attempts to use the CO containing complex **5** for H_2O oxidation, with $[Ru(bpy)_3]^{3+}$ as oxidant, failed, with no detectable amounts of generated O_2 (Figure 2 and Figure S6). Also when Ce^{IV} was used as oxidant no O_2 was produced (compared to complex **4** which was able to produce O_2). This was clearly surprising since oxidation of coordinated CO to CO_2 has frequently been used in iron CO chemistry to form an empty coordination site.[15] In addition, efficient iridium-based WOCs which contain CO have been reported.[6a] The iridium WOCs have been reported to lose the CO ligand by irreversible oxidation (to CO_2), leaving an empty coordination site for an aqua ligand in the oxidation of H_2O. This different behavior of ruthenium and iridium is enticing and highlights a key catalytic divergence among metal-based WOCs. These observations and insights might thus shed light on the deactivation of ruthenium-based WOCs.

Electrochemical measurements were performed on the two single-site ruthenium complexes under relevant catalytic turnover conditions (neutral pH) to understand the striking difference in the reactivity exhibited by complexes **4** and **5**. This would also give further insight into the catalytically active species and the mechanism of the oxidation of water. The differential pulse voltammograms (DPVs) of the complexes at pH 7.2 (0.1 M phosphate buffer/acetonitrile 95:5) provide further insight into their redox chemistry (Figure S17). Complex **4** displayed peaks at +0.15, 0.70, and 0.98 V versus the normal hydrogen electrode (NHE) corresponding to the formal oxidation reactions of $Ru^{II} \rightarrow Ru^{III} \rightarrow Ru^{IV} \rightarrow Ru^{VI}$. The catalytic oxidation of water occurs after the $Ru^{IV} \rightarrow Ru^{VI}$ process, thus affirming that the Ru^{VI} oxidation state initiates the evolution of oxygen. By contrast, complex **5** only shows a single peak at 0.89 V corresponding to the formation of a high-valent ruthenium species. Obviously, the axial ligands have a great influence on the level of π-backbonding in the two complexes, thus reflecting the stability of the ruthenium(III) redox levels and also the reactivity difference towards the catalytic oxidation of H_2O.

The cyclic voltammogram for complex **4**, obtained in an aqueous solution at neutral pH (Figure S19) displays a catalytic current for the oxidation of H_2O starting at about 1.23 V vs. NHE. This onset potential is shifted to higher anodic potentials for complex **5** ($E > 1.28$ V vs. NHE). The oxidant $[Ru(bpy)_3]^{3+}$ delivers a potential of 1.26 V vs. NHE, thus making it thermodynamically unfavorable to drive H_2O oxidation by complex **5**.

DPV measurements of complex **4** in acidic medium (pH 1) also resulted in three well-separated peaks (Figure S18), where two of them are shifted to a more positive potential compared to the potential at pH 7. The first oxidation process at 0.17 V, ascribed to the Ru^{III}/Ru^{II} redox couple, is slightly affected. The second and third oxidation processes at 0.98 and 1.21 V, corresponding to the formal oxidations of $Ru^{III} \rightarrow Ru^{IV} \rightarrow Ru^{VI}$, are shifted to higher potentials. This means that these oxidation reactions are associated with the loss of a proton, that is, these processes are proton-coupled electron transfer (PCET) processes. For complex **5**, the previously observed, single wave at neutral pH, splits into two waves occurring at 0.92 and 1.08 V in acidic medium (pH 1).

To get a more comprehensive insight into the electrochemical properties of complexes **4** and **5**, the dependence of the potentials on the pH (Pourbaix diagrams) for the two complexes were examined in the region $1.5 < pH < 8.0$ (Figure 4). The Pourbaix diagram for complex **4** (Figure 4a)

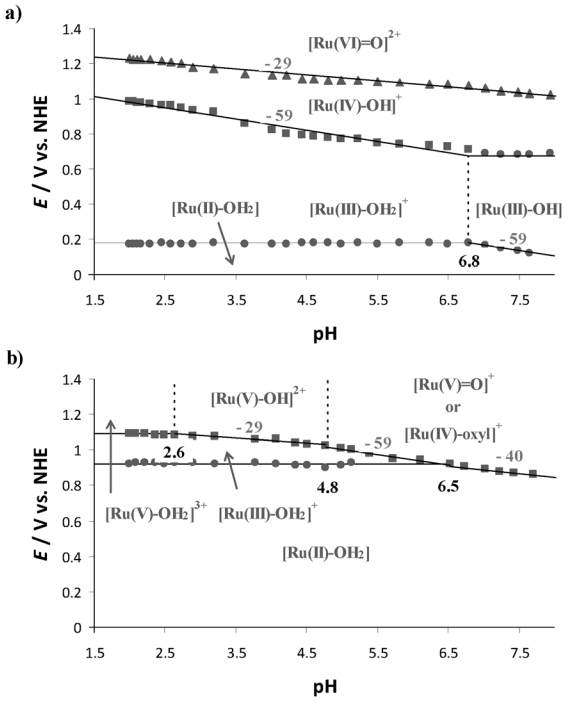

Figure 4. Pourbaix diagrams of a) complex **4** and b) complex **5**, in the range $1.5 < pH < 8.0$ (pK_a values are denoted by the vertical dashed lines). Experimental conditions: Pourbaix diagrams of complexes **4** and **5** (30 μM) were obtained from DPV measurements, in a 0.1 M Britton-Robinson buffer solutions in the range of $1.5 < pH < 8.0$. The pH of the solution was changed by using a 0.2 M NaOH aqueous solution.

reveals that the potential for the Ru^{III}/Ru^{II} couple (0.17 V vs. NHE) is pH independent from pH 1.5 up to 6.8. At pH > 6.8 the potential for the Ru^{III}/Ru^{II} couple follows a Nernstian behavior, where the slope is equivalent to $-(m/n)\cdot 59$ mV per pH unit (where m and n are equivalent to the number of protons and electrons transferred, respectively). The slope was found to be −59 mV/pH and reveals that the one-electron oxidation is accompanied by the transfer of a proton (PCET), ascribed to the $[Ru^{III}\text{-}OH]/[Ru^{II}\text{-}OH_2]$ redox couple.

From the Pourbaix diagram it could thus be determined that the pK_a value for the ruthenium–aqua complex, $[Ru^{III}\text{-}OH_2]^+$, is 6.8. This pH dependent oxidation of complex **4** signals that coordination of H_2O occurs to the low valent ruthenium center (Ru^{II}) as a seventh ligand, perhaps because of the large bite angle (115°) offered by the tetradentate bpb^{2-} ligand. This coordination provides the ruthenium center with easy access to high-valent ruthenium species through PCET events, without ligand exchange. By contrast, the Ru^{IV}/Ru^{III} redox couple is pH dependent in the whole region from pH 1.5 to 6.8, also with a slope of −59 mV per pH unit, corresponding to the formation of $[Ru^{IV}\text{-}OH]^+$. In fact, this species could be detected by HRMS (Figure S12). The next process, the oxidation of $[Ru^{IV}\text{-}OH]^+$ is unique, in the sense that this process has a slope of −29 mV per pH unit over the whole pH range ($1.5 < pH < 8.0$) and is thus a one-proton-two-electron redox process. This actually suggests that a ruthenium(VI)-oxo ($[Ru^{VI}{=}O]^{2+}$) or ruthenium(V)-oxyl species ($[Ru^{V}\text{-oxyl}]^{2+}$), is generated and involved in the catalytic cycle of H_2O oxidation. This differs from a majority of the reported catalysts for H_2O oxidation, in which the catalysts usually are oxidized to the ruthenium(V) state, which is the catalytically important intermediate.

The Pourbaix diagram of complex **5** is different from that of complex **4**, and contains peculiar features (Figure 4b). The first redox process, assigned to the $[Ru^{III}\text{-}OH_2]^+/[Ru^{II}\text{-}OH_2]$ couple, is pH independent over a wide range of proton concentrations (from pH 1.5 up to pH 6.5). The next oxidation process displays a complex behavior over the studied pH range. In the region of pH 1.5–2.6 the potential of this process is pH independent and is assumed to involve a two-electron oxidation process, corresponding to $[Ru^{V}\text{-}OH_2]^{3+}/[Ru^{III}\text{-}OH_2]^+$. From pH 2.6 to 4.8, the oxidation changes behavior and has a slope of −29 mV per pH unit, implying that this process is now a one-proton-two-electron oxidation to form the species $[Ru^{V}\text{-}OH]^{2+}$. Between pH 4.8–6.5 the dependence of the potential has a slope of −59 mV per pH unit and corresponds to a two-proton-two-electron-oxidation involving the redox couple $[Ru^{V}{=}O]^+/[Ru^{III}\text{-}OH_2]^+$. At pH > 6.5 the Pourbaix diagram has a slope of −40 mV per pH unit and astonishingly hints that this process is a two-proton-three-electron oxidation and that it is possible to directly go from $[Ru^{II}\text{-}OH_2]$ to $[Ru^{V}{=}O]^+$. The difference in reactivity towards H_2O oxidation for complexes **4** and **5** could be explained by assuming that it is necessary to reach the ruthenium(VI) state to obtain a species capable of oxidizing H_2O. The production of the species $[Ru^{VI}{=}O]^{2+}$ at relatively low redox potential for complex **4**, may be the reason why it displays catalytic activity in H_2O oxidation.

For complex **4**, a kinetic study was performed, where the initial rate of O_2 formation was found to be first-order in the catalyst concentration (Figures S8 and S9), suggesting that bimolecular reactions do not contribute to the catalytic H_2O oxidation. Based on the kinetics of the catalysis with complex **4**, together with the electrochemical results, we suggest a mononuclear mechanism with the involvement of a $[Ru^{VI}{=}O]$ species. The key structural feature of complex **4** is the large bite angle of 115° provided by the tetradentate ligand **3**, allowing for easy access of an aqua ligand to the metal center. For complex **4**, the first oxidation process furnishes a seven-coordinated $[Ru^{IV}\text{-}OH]^+$ species through a proton-coupled electron event (at neutral pH). This one-electron species was also detected by HRMS, after the addition of 4 equivalents of the oxidant $[Ru(bpy)_3]^{3+}$ to a solution containing **4** (Figure S12). The subsequent oxidation process is also proton-coupled and is assumed to generate a $[Ru^{VI}{=}O]^{2+}$ intermediate, the crucial species for H_2O oxidation catalysis. This highly electrophilic $[Ru^{VI}{=}O]^{2+}$ species presumably undergoes a nucleophilic attack by a water molecule, accompanied by loss of a proton, to generate a hydroperoxo species $[Ru^{IV}\text{-}OOH]^+$.[16] A further proton-coupled oxidation step then furnishes the fragment $[Ru^{V}\text{-}OO]^+$ which liberates molecular O_2 and regenerates the starting Ru^{III} species.

To conclude, the examination of the two related single-site ruthenium complexes **4** and **5** containing the easily accessible and modifiable tetradentate ligand scaffold H_2bpb (**3**), reveals striking differences in the reactivity of the two complexes. While complex **4** is an efficient catalyst for the oxidation of water, **5** turns out to be inactive. The fact that complex **5** is formed from **4** under catalytic conditions is a key observation and an important feature in the search for more stable and efficient WOCs. The difference in the electrochemical properties of the two structurally similar single-site ruthenium complexes is intriguing and highlights the strong impact exerted by the axial ligands on the catalytic activity of the ruthenium centers. Ease of access of an aqua ligand to the metal center is important for WOCs but although complex **5** has relatively low oxidation potentials and contains an axially coordinated aqua ligand, this does not result in an active WOC. Recognition of these features constitutes a basic design principle for the development of future WOCs.

Received: December 21, 2012
Published online: March 14, 2013

Keywords: energy conversion · homogeneous catalysis · oxidation of water · oxygen evolution · ruthenium

[1] a) L. Sun, L. Hammarström, B. Åkermark, S. Styring, *Chem. Soc. Rev.* **2001**, *30*, 36–49; b) M. Hambourger, G. F. Moore, D. M. Kramer, D. Gust, A. L. Moore, T. A. Moore, *Chem. Soc. Rev.* **2009**, *38*, 25–35.

[2] Y. Umena, K. Kawakami, J.-R. Shen, N. Kamiya, *Nature* **2011**, *473*, 55–60.

[3] a) H. Dau, C. Limberg, T. Reier, M. Risch, S. Roggan, P. Strasser, *ChemCatChem* **2010**, *2*, 724–761; b) F. Jiao, H. Frei, *Energy Environ. Sci.* **2010**, *3*, 1018–1027.

[4] a) M. W. Kanan, D. G. Nocera, *Science* **2008**, *321*, 1072 – 1075; b) M. Risch, V. Khare, I. Zaharieva, L. Gerencser, P. Chernev, H. Dau, *J. Am. Chem. Soc.* **2009**, *131*, 6936 – 6937; c) F. Jiao, H. Frei, *Angew. Chem.* **2009**, *121*, 1873 – 1876; *Angew. Chem. Int. Ed.* **2009**, *48*, 1841 – 1844.

[5] a) S. W. Gersten, G. J. Samuels, T. J. Meyer, *J. Am. Chem. Soc.* **1982**, *104*, 4029 – 4030; b) Y. V. Geletii, C. Besson, Y. Hou, Q. Yin, D. G. Musaev, D. Quiñonero, R. Cao, K. I. Hardcastle, A. Proust, P. Kögerler, C. L. Hill, *J. Am. Chem. Soc.* **2009**, *131*, 17360 – 17370; c) Y. Xu, A. Fisher, L. Duan, L. Tong, E. Gabrielsson, B. Åkermark, L. Sun, *Angew. Chem.* **2010**, *122*, 9118 – 9121; *Angew. Chem. Int. Ed.* **2010**, *49*, 8934 – 8937; d) M. D. Kärkäs, E. V. Johnston, E. A. Karlsson, B.-L. Lee, T. Åkermark, M. Shariatgorji, L. Ilag, Ö. Hansson, J.-E. Bäckvall, B. Åkermark, *Chem. Eur. J.* **2011**, *17*, 7953 – 7959; e) Y. Xu, L. Duan, T. Åkermark, L. Tong, B.-L. Lee, R. Zhang, B. Åkermark, L. Sun, *Chem. Eur. J.* **2011**, *17*, 9520 – 9528; f) M. D. Kärkäs, T. Åkermark, E. V. Johnston, S. R. Karim, T. M. Laine, B.-L. Lee, T. Åkermark, T. Privalov, B. Åkermark, *Angew. Chem.* **2012**, *124*, 11757 – 11761; *Angew. Chem. Int. Ed.* **2012**, *51*, 11589 – 11593; g) L. Duan, F. Bozoglian, S. Mandal, B. Stewart, T. Privalov, A. Llobet, L. Sun, *Nat. Chem.* **2012**, *4*, 418 – 423.

[6] a) J. D. Blakemore, N. D. Schley, D. Balcells, J. F. Hull, G. W. Olack, C. D. Incarvito, O. Eisenstein, G. W. Brudvig, R. H. Crabtree, *J. Am. Chem. Soc.* **2010**, *132*, 16017 – 16029; b) D. G. H. Hetterscheid, J. N. H. Reek, *Chem. Commun.* **2011**, *47*, 2712 – 2714.

[7] a) Y. Gao, T. Åkermark, J. Liu, L. Sun, B. Åkermark, *J. Am. Chem. Soc.* **2009**, *131*, 8726 – 8727; b) R. Brimblecombe, A. Koo, G. C. Dismukes, G. F. Swiegers, L. Spiccia, *J. Am. Chem. Soc.* **2010**, *132*, 2892 – 2894; c) E. A. Karlsson, B.-L. Lee, T. Åkermark, E. V. Johnston, M. D. Kärkäs, J. Sun, Ö. Hansson, J.-E. Bäckvall, B. Åkermark, *Angew. Chem.* **2011**, *123*, 11919 – 11922; *Angew. Chem. Int. Ed.* **2011**, *50*, 11715 – 11718.

[8] a) W. C. Ellis, N. D. McDaniel, S. Bernhard, T. J. Collins, *J. Am. Chem. Soc.* **2010**, *132*, 10990 – 10991; b) J. L. Fillol, Z. Codolà, I. Garcia-Bosch, L. Gómez, J. J. Pla, M. Costas, *Nat. Chem.* **2011**, *3*, 807 – 813.

[9] a) Z. Huang, Z. Luo, Y. V. Geletii, J. W. Vickers, Q. Yin, D. Wu, Y. Hou, Y. Ding, J. Song, D. G. Musaev, C. L. Hill, T. Lian, *J. Am. Chem. Soc.* **2011**, *133*, 2068 – 2071; b) S. Tanaka, M. Annaka, K. Sakai, *Chem. Commun.* **2012**, *48*, 1653 – 1655; c) D. J. Wasylenko, C. Ganesamoorthy, J. Borau-Garcia, C. P. Berlinguette, *Chem. Commun.* **2011**, *47*, 4249 – 4251.

[10] a) F. Liu, T. Cardolaccia, B. J. Hornstein, J. R. Schoonover, T. J. Meyer, *J. Am. Chem. Soc.* **2007**, *129*, 2446 – 2447; b) J. Mola, E. Mas-Marza, X. Sala, I. Romero, M. Rodríguez, C. Viñas, T. Parella, Antoni Llobet, *Angew. Chem.* **2008**, *120*, 5914 – 5916; *Angew. Chem. Int. Ed.* **2008**, *47*, 5830 – 5832.

[11] D. J. Wasylenko, C. Ganesamoorthy, B. D. Koivisto, M. A. Henderson, C. P. Berlinguette, *Inorg. Chem.* **2010**, *49*, 2202 – 2209.

[12] B.-L. Lee, M. D. Kärkäs, E. V. Johnston, A. K. Inge, L.-H. Tran, Y. Xu, Ö. Hansson, X. Zou, B. Åkermark, *Eur. J. Inorg. Chem.* **2010**, 5462 – 5470.

[13] a) D. J. Barnes, R. L. Chapman, R. S. Vagg, E. C. Watton, *J. Chem. Eng. Data* **1978**, *23*, 349 – 350; b) O. Belda, C. Moberg, *Coord. Chem. Rev.* **2005**, *249*, 727 – 740.

[14] a) Y. V. Geletii, B. Botar, P. Kögerler, D. A. Hillesheim, D. G. Musaev, C. L. Hill, *Angew. Chem.* **2008**, *120*, 3960 – 3963; *Angew. Chem. Int. Ed.* **2008**, *47*, 3896 – 3899; b) Q. Yin, J. M. Tan, C. Besson, Y. V. Geletii, D. G. Musaev, A. E. Kuznetsov, Z. Luo, K. I. Hardcastle, C. L. Hill, *Science* **2010**, *328*, 342 – 345.

[15] a) W. Gao, J. Ekström, J. Liu, C. Chen, L. Eriksson, L. Weng, B. Åkermark, L. Sun, *Inorg. Chem.* **2007**, *46*, 1981 – 1991; b) S. Ezzaher, J.-F. Capon, F. Gloaguen, F. Y. Pétillon, P. Schollhammer, J. Talarmin, *Inorg. Chem.* **2007**, *46*, 3426 – 3428.

[16] a) J. J. Concepcion, M.-K. Tsai, J. T. Muckerman, T. J. Meyer, *J. Am. Chem. Soc.* **2010**, *132*, 1545 – 1557; b) D. J. Wasylenko, C. Ganesamoorthy, M. A. Henderson, C. P. Berlinguette, *Inorg. Chem.* **2011**, *50*, 3662 – 3672.

